JOURNAL OF BACTERIOLOGY, Sept. 1983, p. 1288–1296
0021-9193/83/091288-09$02.00/0

Vol. 155, No. 3

Structure and Function of the Internal Promoter (*hisBp*) of the *Escherichia coli* K-12 Histidine Operon

VINCENZA GRISOLIA, ANDREA RICCIO, AND CARMELO B. BRUNI*

Centro di Endocrinologia ed Oncologia Sperimentale del Consiglio Nazionale delle Ricerche and Cattedra di Microbiologia, Istituto di Patologia Generale, II Facoltà di Medicina, University of Naples, 80131 Naples, Italy

Received 8 April 1983/Accepted 30 June 1983

The entire histidine operon of *Escherichia coli* K-12 was cloned in the vector plasmid pBR313, and a complete restriction map of the operon was determined. By using subclones, complementation tests, and enzyme assays, we were able to make a correlation between the physical map and the genetic map of the operon. We determined the sequence of a fragment of DNA 665 base pairs long, comprising the distal portion of the *hisC* gene, the proximal portion of the *hisB* gene, and the internal transcription initiation site *hisBp*. The efficiency of this promoter was assessed under different physiological conditions by cloning the DNA fragment in a recombinant vector system used to study transcriptional regulatory signals. The precise point at which transcription initiates was determined by S1 nuclease mapping.

Our laboratory has been interested for the past few years in the study of the biosynthetic histidine operon of *Escherichia coli* K-12. Several features of the proximal region of this operon and the mechanism of coupled translation-transcription termination (attenuation) by which the operon expression is regulated have been analyzed and are summarized in reference 4. In an attempt to better define the still poorly known features of the distal portion of this operon, we previously reported the cloning of this region of the *E. coli* K-12 chromosome comprising the *hisBHAFI(E)* genes and the mapping of an internal transcription initiation site (18). We have now extended these studies and report here the cloning, in a vector plasmid, and the restriction map of the entire operon, the location of several genes by subcloning and complementation tests, the sequence of a DNA fragment comprising the end of the *hisC* gene and the beginning of the *hisB* gene, and the structure and function of the internal *hisBp* promoter.

MATERIALS AND METHODS

Bacterial strains and plasmids. The bacterial strains used are listed in Table 1. Construction of plasmids pCB3 (7) and pVG2, pVG4, and pVG5 (18) has already been described. The multicopy plasmids pK01, pK04, and pKG1800 (26) were obtained from M. Rosenberg. Details of the construction of histidine recombinant plasmids pHC9800 and pHC665 are given below.

Media, growth conditions, and enzyme assays. Liquid media were LB broth (27) and minimal medium (35) supplemented with 0.5% glucose. Solid media contained 1.2% agar (Difco Laboratories, Detroit, Mich.) and were nutrient broth (27) and minimal medium (35) supplemented with 0.5% glucose. Amino acids were added at 0.5 mM; L-histidine was added at 0.1 mM. Derepression of the histidine operon was obtained by adding 3-amino-1,2,4-triazole (6) to logarithmically growing cells in the presence of 0.4 mM adenine. Tetracycline and ampicillin were added to both liquid and solid media at 25 and 50 μg/ml, respectively. Strains for enzyme assays or for RNA preparation were grown to an absorbance at 650 nm of 0.8. Assay procedures for the enzymes of the histidine pathway (histidinol phosphatase [E.C. 3.1.3.15; B enzyme] and imidazolylacetol-phosphate:L-glutamate aminotransferase [E.C. 2.6.1.9; C enzyme]) have been described elsewhere (23). The assay for galactokinase (E.C. 2.7.1.6) was performed as described elsewhere (26). Proteins were measured by the method of Lowry et al. (21).

Chemicals and enzymes. All amino acids, histidinol phosphate, and glyoxal were obtained from Sigma Chemical Co., St. Louis, Mo. Acrylamide, methylenebisacrylamide, ammonium persulfate, *N,N,N',N'*-tetramethylenediamine, and agarose were from Bio-Rad Laboratories, Richmond, Calif. Guanidine hydrochloride was from Bethesda Research Laboratories, Bethesda, Md. [γ-^{32}P]ATP (3,000 Ci/mmol) was from Amersham Corp., Arlington Heights, Ill. Restriction endonucleases *Hpa*I, *Pst*I, *Sal*I, *Sma*I, and *Hae*III were purchased from Bethesda Research Laboratories. *Hin*dIII, *Bam*HI, *Hin*fI, *Alu*I, *Hpa*II, *Bst*NI, *Taq*I, *Mbo*II, *Hga*I, and *Eco*RI were from New England Biolabs, Beverly, Mass. *Bgl*II was purified as described previously (3). Calf intestine alkaline phosphatase was from Boehringer Mannheim Corp., New

TABLE 1. *E. coli* K-12 strains[a]

Strain	Genotype	Source or construction
FB1	Δ(*hisGDCBHAFIE*)*750 gnd rhaA*	Garrick-Silversmith and Hartman (14)
FB8	Wild-type *E. coli* K-12, UTH1038	Kasai (20)
FB181	*hisI903*	Goldschmidt et al. (15)
FB182	*hisF892*	Goldschmidt et al. (15)
FB184	*hisA915*	Goldschmidt et al. (15)
FB190	*hisG2743 recA56*	Bruni et al. (7)
FB194	*hisG2743 recA56* (pCB3)	Bruni et al. (7)
FB251	*hisB855 recA56*	Grisolia et al. (18)
FB252	*hisB855 recA56* (pVG2)	Grisolia et al. (18)
FB254	*hisB855 recA56* (pVG4)	Grisolia et al. (18)
FB255	*hisB855 recA56* (pVG5)	Grisolia et al. (18)
FB256	Δ(*hisGDCBHAFIE*)*750 gnd rhaA* (pVG2)	Grisolia et al. (18)
FB257	Δ(*hisGDCBHAFIE*)*750 gnd rhaA* (pHC9800)	This paper
FB266	Δ(*hisGDCBHAFIE*)*750 gnd rhaA* (pVG4)	This paper
FB267	*galK2 recA13* (pKO4)	Mc Kenney et al. (26)
FB268	*galK2 recA13* (pKG1800)	Mc Kenney et al. (26)
FB269	*galK2 recA13* (pAR1)	This paper
FB270	*galK2 recA13* (pHC665)	This paper
N100	*galK2 recA13*	Mc Kenney et al. (26)

[a] Genetic symbols are those given by Bachmann and Low (2).

York, N.Y.; T4 polynucleotide kinase and ligase were from Miles Laboratories, Inc., Elkhart, Ind.; and S1 nuclease was from Sigma. Either unlabeled or ^{32}P-labeled pBR322, digested with *Hin*fI, was used as a standard of molecular weight on acrylamide gels. *Hin*dIII digests of λ DNA were used as molecular-weight standards on agarose gels.

DNA fractionation and labeling. Plasmid DNA was prepared as described elsewhere (8). For screening large numbers of transformants, plasmid DNA was purified by a rapid method described elsewhere (9). DNA fragments were isolated on and purified from preparative 5% acrylamide slab gels by electroelution as described elsewhere (22). 5'-Terminal labeling of DNA fragments was performed with T4 polynucleotide kinase and [γ-^{32}P]ATP, as described elsewhere (25), except that calf intestine alkaline phosphatase was used instead of bacterial alkaline phosphatase and the enzyme was inactivated by heating for 10 min at 75°C.

Restriction maps. The restriction map of the plasmid DNA was determined by using restriction sites uniquely present in the vector or cloned DNA, as described below. Fine mapping of the *Hin*dIII-*Bgl*II 665-base pair (bp) fragment was performed by double digestions with *Hin*fI and several other restriction enzymes.

Cloning and transformation. Plasmid pHC9800 was obtained by mixing plasmid pVG2 and pCB3 DNAs, both restricted with *Hin*dIII. The DNA mixtures were ligated and used to transform strain FB1, as previously described (7). Plasmid pHC665 was obtained by cloning the purified 665-bp *Hin*dIII-*Bgl*II fragment in the vector pKO4, restricted with *Hin*dIII and *Bam*HI. Details of the construction of pHC665 are given below. The presence and the estimated copy number of plasmids in transformed cells used for enzyme assays were checked as previously described (7).

RNA preparation and S1 mapping. Total RNA was extracted from *E. coli* FB256 by the guanidine hydrochloride procedure (16) modified as previously described (18). RNA-DNA hybridizations, S1 nuclease digestion, and analysis of hybrids on denaturing gels were performed as described elsewhere (12). The reaction mixtures contained 200 ng of 5'-labeled DNA probe (specific activity, 500,000 cpm/μg) and 40 μg of specific RNA. S1 nuclease digestion was for 1 h at 37°C with 100 U of enzyme per assay. Products were analyzed on 8% acrylamide slab gels in 7 M urea and visualized by autoradiography, using Kodak X-Omat R films exposed at −80°C.

DNA sequencing. DNA sequencing was performed by the technique of Maxam and Gilbert (25). The 665-bp *Hin*dIII-*Bgl*II fragment, as such or digested with several restriction enzymes, was terminally labeled at the 5' ends. Fragments labeled at only one end were obtained either by strand separation or by secondary restriction enzyme cleavage as described elsewhere (25).

RESULTS

Cloning of the entire *his* operon and localization of genes by transformation and complementation tests. The entire *his* operon of *E. coli* K-12 was cloned by recombining in vitro the proximal portion of the operon contained in plasmid pCB3 to the distal one contained in plasmid pVG2. pCB3 contains the proximal *hisG* and *hisD* genes (7), and pVG2 contains the distal *hisBHAFI* and possibly *hisE* genes (18). The two plasmids are pBR313 derivatives and have a *Hin*dIII insert 5,300 and 4,500 bp long, respectively (Fig. 1). Plasmid DNAs were restricted with *Hin*dIII, mixed in equimolar amounts, and religated. The DNA mixture was used to transform the *E. coli* K-12 strain FB1 containing a complete deletion of the *his* operon. Transformants were selected on LB ampicillin plates and scored for growth on

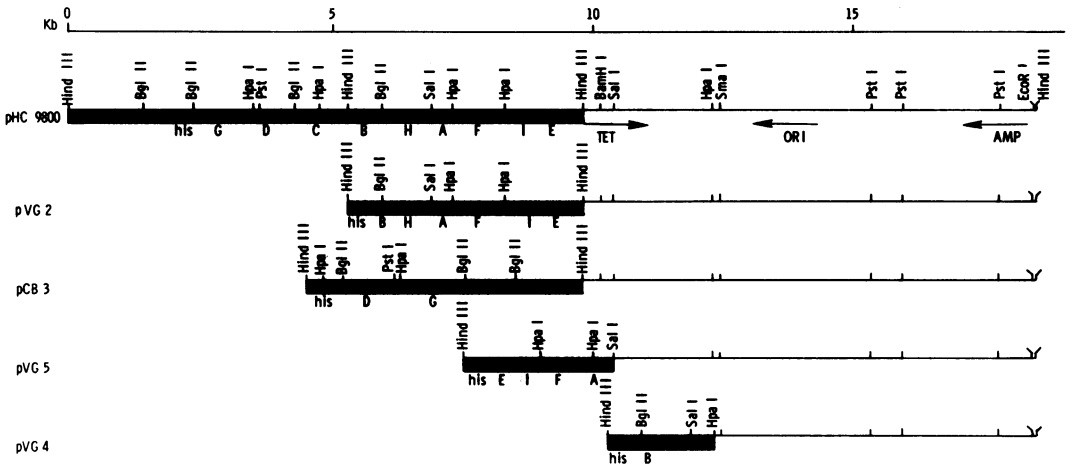

FIG. 1. Physical map of the recombinant histidine plasmids. The circular plasmid DNAs are schematically linearized at the unique *Hin*dIII site of vector pBR313. The filled bars represent fragments cloned. The arrows indicate the orientation of the tetracycline-resistant genes (TET), the origin of replication (ORI), and the ampicillin-resistant gene (AMP). Plasmid pVG2 containing the distal *hisBHAFIE* genes (18) and pCB3 containing the proximal *hisGD* genes (7) have already been described. Pasmid pVG4 contains the 2,000-bp *Hin*dIII-*Hpa*I proximal fragment derived from pVG2 and carries a complete *his*B gene. Plasmid pVG5 contains the 2,900-bp *Sal*I-*Hin*dIII distal fragment, with respect to the pVG2 map, and carries the *hisAFIE* distal genes. Plasmid pHC9800 contains the complete histidine operon; details of its construction are given in the text. Kb, Kilobases.

minimal medium. Several minimal growers, ampicillin-resistant clones, were found and analyzed by rapid plasmid isolation. All of them contained a 18,500-bp plasmid (pHC9800) which, upon digestion with *Hin*dIII, gave rise to three fragments of 8,700, 5,300 and 4,500 bp, respectively (Fig. 2). The 8,700-bp fragment represents the pBR313 vector, and the 5,300-bp fragment represents the proximal part and the 4,500 bp the distal part of the *his* operon. Digestion with *Bgl*II showed the bands already present in the two parent plasmids (7, 18) and a new 1,600-bp fragment spanning the internal *Hin*dIII site (Fig. 2). These results allowed the construction of a complete restriction map of the *E. coli* K-12 *his* operon contained in plasmid pHC9800 (Fig. 1). The *hisC* gene product is missing in strains harboring both parental plasmids (7, 18). Fusion of the *Hin*dIII fragments in plasmid pHC9800 (Fig. 1) must have also reconstituted an intact *hisC* gene, since plasmid pHC9800 conferred a His^+ phenotype to strain FB1 containing a complete *his* deletion. To further prove this point, we measured the *hisC* enzyme levels in the plasmid-harboring strain FB257. As shown in Table 2, the enzyme levels were quite high compared with those of a wild-type strain (about 30-fold) and compatible with the presence of a multicopy plasmid (5, 19). Enzyme levels were elevated in both rich and minimal medium. At variance with the wild-type strain FB8, the addition of 3-amino-1,2,4-triazole up to 50 mM could not induce derepression of the *his* operon in strain FB257 due to the high basal levels of *hisB* enzyme which make the inhibitor ineffective, as evidenced by the minimal decrease in growth rate (Table 2).

To map the *his* genes on individual DNA fragments, we made use of the several available subclones shown in Fig. 1. These plasmids were used to transform several *his* mutants on LB ampicillin plates, and then 50 clones from each transformation were tested for growth in minimal medium (Table 3). The *hisBp* promoter and the *hisB* gene were localized on the *Hin*dIII-*Hpa*I 2,000-bp DNA fragment cloned in plasmid pVG4 (Fig. 1). The presence of a complete *hisB* gene on the *Hin*dIII-*Hpa*I 2,000-bp fragment was confirmed by performing enzyme assays on strains harboring the plasmids (Table 2). The enzyme levels of strains FB256 and FB266 harboring pVG2 and pVG4 plasmids, respectively, were very similar. Moreover, the presence of pVG4 confers to recipient strain FB251 a His^+ phenotype (18; Table 3). Since FB251, which still retains the phosphatase activity, is mutated in the carboxy-terminal dehydratase moiety of the bifunctional *hisB* gene product (18, 33; Table 2), the cloned fragment must also contain the genetic information for this activity. The *hisAFIE* genes are localized on the *Sal*I-*Hin*dIII 2,900-bp DNA fragment cloned in plasmid pVG5 (Fig. 1). The location of the *hisH* gene was not established for lack of appropriate mutants.

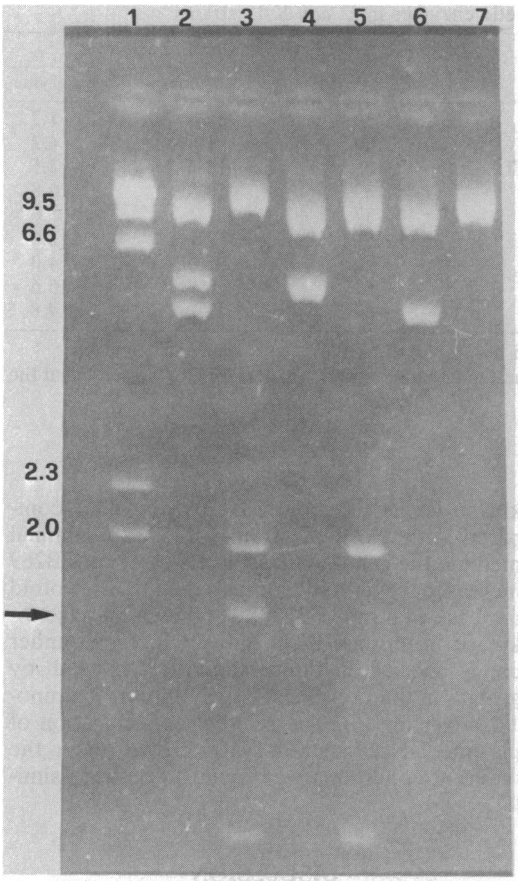

FIG. 2. Restriction pattern of histidine recombinant plasmid DNA; 1.5% agarose slab gel of pHC9800, pCB3, and pVG2 DNA digested with *Hin*dIII or *Bgl*II. Lane 1, λ DNA digested with *Hin*dIII and used as marker; the size in kilobases of some of the fragments is indicated. Lanes 2, 4, and 6, pHC9800, pCB3, and pVG2 DNA digested with *Hin*dIII, showing both the 5,300- and 4,500-bp fragments, only the 5,300-bp fragment, and only the 4,500-bp fragment, respectively. Lanes 3, 5, and 7, pHC9800, pCB3, and pVG2 DNA, respectively, digested with *Bgl*II. pHC9800 contains the new 1,600-bp band (arrow) generated by fusion of the two *Hin*dIII fragments. Both pHC9800 and pCB3 contain the two internal fragments of 2,000 and 900 bp, respectively, whereas pVG2, containing only one *Bgl*II site is linearized.

Expression of the *hisAFI* genes in plasmid pVG5, which does not contain the *hisBp* promoter (18), must be under the control of a plasmid promoter or of a hitherto unrecognized internal promoter or be due to a gene dosage effect of the multicopy plasmid in the presence of a low spurious transcription initiation site.

Structure of the internal *hisBp* promoter and flanking regions. In the absence of the primary *hisGp* promoter, the distal *his* genes are expressed from an internal promoter (1, 11, 18) which is localized on the *Hin*dIII-*Bgl*II 665-bp DNA fragment (18; Fig. 1). To study this promoter in more detail, we sequenced this region of DNA. We first determined a detailed restriction map (Fig. 3) along with the sequencing strategy adopted. The complete sequence of the 665-bp DNA fragment is shown in Fig. 4. As previously inferred (7), this fragment should contain approximately the last 400 bp of the *hisC* gene. By analyzing the three possible reading frames 5′ to 3′, two were terminated at nucleotides 66 to 68 and 244 to 246, respectively, by TGA stop codons (Fig. 4). The third reading frame was open up to nucleotide 427, and the putative peptide ended with two tandem TGA stop codons. Further down along the sequence, the only open reading frame to the end of the fragment started with the methionine codon at nucleotides 430 to 432, which spans the two TGA stop codons at the end of *hisC*. This putative amino acid sequence could define the amino terminal region of the *hisB* protein.

To more precisely locate the internal transcription initiation site, single-strand nuclease mapping analysis was carried out together with DNA sequencing experiments (Fig. 5). RNA was extracted from strain FB256, carrying a complete *his* deletion and harboring the distal *his* plasmid pVG2, and hybridized to the *Bst*NI-*Hpa*II DNA fragment terminally labeled at the 5′ end in the *Hpa*II site at nucleotide 532 of Fig. 4. After S1 digestion, mainly two fragments, differing in length by one nucleotide, were visible on the denaturing slab gel (Fig. 5, lane 1). The same labeled fragment was sequenced, and the products were run in parallel to generate markers (Fig. 5, lane 2). Taking into account the fact that the guanine ladder shown in Fig. 5 represents the sequence of the coding strand and making a correction of 1.5 nucleotides (32), it could be deduced that transcription from the *hisBp* promoter initiated at nucleotides 322 and 323 of the sequence shown in Fig. 4.

Function of the *hisBp* promoter. The function of the *hisBp* promoter was investigated in a vector system specifically constructed for the study of transcription regulatory signals (26). The vector plasmids pKO1 and pKO4 contain a *galK* gene which is very poorly expressed, since no strong promoter for *galK* is present (26; Table 4). Upstream of the *galK* gene, pKO1 contains unique sites for *Hin*dIII and *Sma*I, which can be used to insert DNA fragments carrying promoter sequences. pKO4 is identical except for the presence of a *Bam*HI site inserted (on a linker) at the *Sma*I target of pKO1. Insertion of promoters induces expression of the *galK* gene, and the recombinants can be identified by

TABLE 2. Levels of histidine biosynthetic enzymes in *E. coli* K-12 strains

Strain	Relevant genotype	Medium	Generation time (min)	Enzyme level[a]	
				C enzyme	B enzyme
FB8	Wild type	LB	36	0.4	1.2
		Minimal	60	1.6	4.2
		Minimal + 20 mM AT[b]	186	10.7	12.5
FB257	FB1(pHC9800)	LB	39	10.8	20.8
		Minimal	87	61.2	105.6
		Minimal + 50 mM AT[b]	108	77.1	112.0
FB251	*hisB855*	Minimal + His	70	1.6	4.0
FB256	FB1(pVG2)	Minimal + His	60	<0.1	15.6
FB266	FB1(pVG4)	Minimal + His	60	<0.1	14.8

[a] Enzyme-specific activities are expressed as described by Martin et al. (23).
[b] Cells were grown to an absorbance at 650 nm of 0.3, and then 3-amino-1,2,4 triazole (AT) (6) was added at the final molar concentrations indicated.

the "red" phenotype on Gal-MacConkey plates. Additional features ensure that the levels of galactokinase are a direct measure of promoter efficiency (26). The 665-bp *Hin*dIII-*Bgl*II fragment was purified as described above and cloned in the vector pKO4. pKO4 DNA was digested with *Hin*dIII and *Bam*HI, mixed with equimolar amounts of the fragment, and ligated. The mixture was restricted with *Bam*HI to eliminate wild-type pKO4 recombinants and used to transform strain N100. Transformation was performed on Gal-MacConkey plates, and several red colonies were further analyzed. Insertion of the fragment and its orientation were determined by digesting plasmid DNA with *Hae*III (data not shown). The resulting plasmid was named pHC665; its structure is presented in Fig. 6. We compared galactokinase levels of strain N100 harboring plasmid pHC665 (FB270) to those of the same strain harboring plasmids pAR1 (FB269) and pKG1800 (FB268). pAR1 is a pKO1 derivative containing the primary *hisGp* promoter (A. Riccio, C. B. Bruni, and F. Blasi, unpublished data). pKG1800 is a pKO1 derivative containing the *galEp* promoter (26). Enzyme levels were measured under different growth conditions (Table 4). In rich medium the galactokinase levels of strain FB270 were 43% compared with those of strain FB269. In minimal medium the galactokinase levels of strain FB269 increased sevenfold compared with a twofold increase in strain FB270. The levels of galactokinase in strain FB270 did not increase under conditions of histidine limitation caused by growth in the presence of the inhibitor 3-amino-1,2,4-triazole (6). The relative concentration of plasmid DNA in strain N100 grown under the different conditions was found to be very similar.

DISCUSSION

In this paper we report evidence that the joining of two contiguous *Hin*dIII fragments of the bacterial chromosome reconstitutes a functional *hisC* gene. This result enabled us to map the distal portion of the *hisC* gene on the *Hin*dIII-*Bgl*II 665-bp fragment. We determined the nucleotide sequence of this fragment and analyzed the amino acid composition of the putative peptides in the three possible reading frames. Termination codons were present after 65, 243, and 427 nucleotides, respectively. On the basis of size estimates of the *hisC* gene (7,

TABLE 3. Transformation of several *E. coli* K-12 *his* mutants with different histidine plasmids

Plasmid	Transformation					
	FB190 (*hisG*)	FB251 (*hisB*)	FB184 (*hisA*)	FB181 (*hisF*)	FB182 (*hisI*)	FB1 (Δ*his*)
pBR313	−	−	−	−	−	−
pCB3 (*hisGD*)	+	−	−	−	−	NT[a]
pVG2 (*hisBHAFIE*)	−	+	+	+	+	−
pVG4	−	+	−	−	−	−
pVG5	−	−	+	+	+	NT
pHC9800	+	+	+	+	+	+

[a] NT, Not tested.

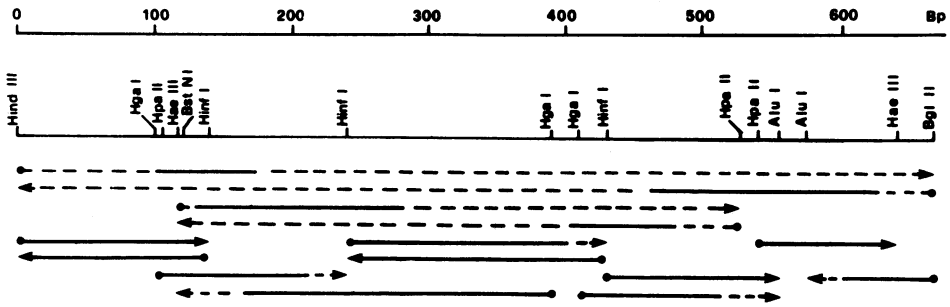

FIG. 3. Restriction endonuclease cleavage sites and sequence strategy of the *Hin*dIII-*Bgl*II 665-bp fragment comprising the end of *hisC*, the beginning of *hisB*, and the internal *hisBp* promoter. The arrows indicate the direction and distance each fragment was sequenced. Broken regions of the arrows signify that the sequence of these regions was not determined in these experiments. Closed circles at the beginning of the arrows indicate the position of the ^{32}P label at the 5′ ends.

18, 24) and the correlation between the genetic map and physical map of the operon (7; Fig. 1), the third open frame more likely represents the true amino acid sequence of the *hisC* protein. Other evidence to support this hypothesis is the following. In this frame the carboxy-terminal amino acid is valine, the same amino acid determined by hydrazinolysis of the purified *Salmonella typhimurium* enzyme (24). At variance with the other two reading frames, this amino

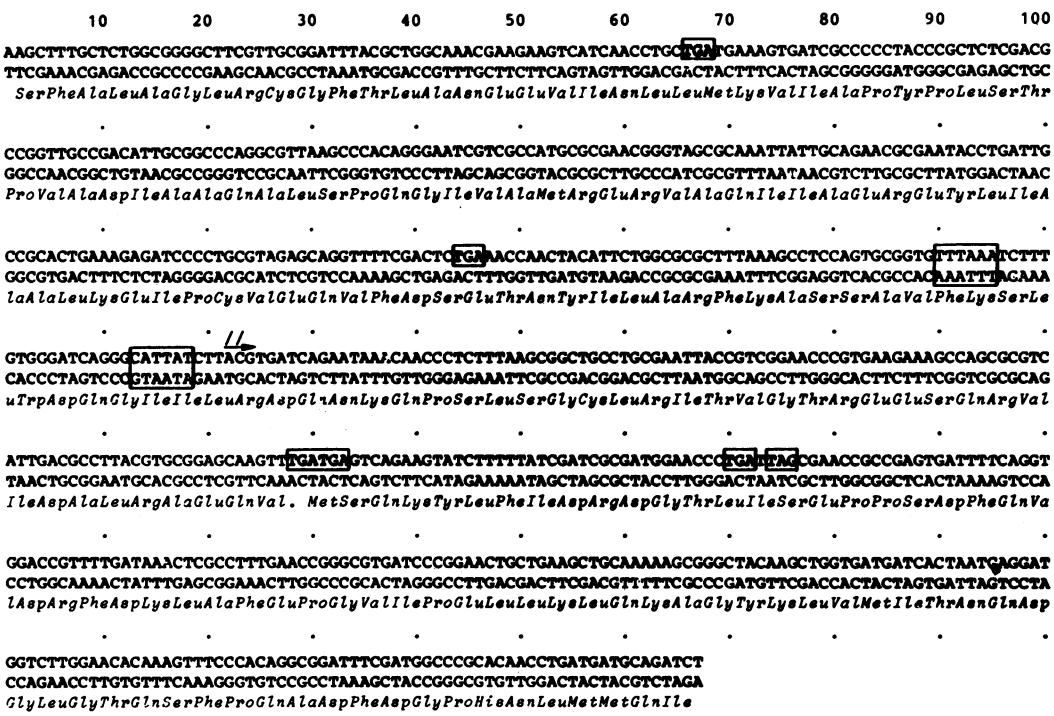

FIG. 4. Nucleotide sequence of the interal *hisBp* promoter and flanking regions. The −35 and −10 consensus sequences are boxed. Nucleotides corresponding to the 5′ end of the mRNA are indicated (↱). The amino acid sequences of the distal portion of *hisC* and proximal portion of *hisB* are shown. The first nonsense codons in the different reading frames are also boxed. Each region of the sequence was determined more than once and on both strands, with the exception of nucleotides 1 to 10 and 140 to 160, which were sequenced only on the noncoding strand, and of nucleotides 405 to 415 and 640 to 667, whose sequence was determined only on the coding strand.

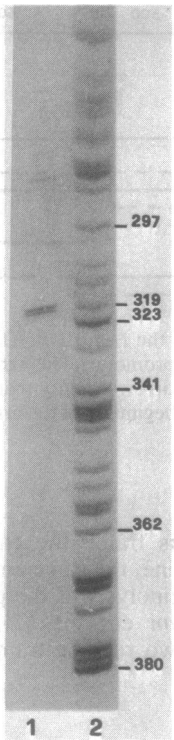

FIG. 5. Localization of the 5' end of the distal *his* mRNA by S1 nuclease gel mapping. The 665-bp *Hin*dIII-*Bgl*II fragment was digested with *Hpa*II, labeled at the 5' end, and recleaved with *Bst*NI. The *Bst*NI-*Hpa*II fragment (nucleotides 122 to 532 of Fig. 4), labeled at the 5' end of the coding strand, was used for sequence determination and S1 mapping. For experimental details, see the text. Lane 1, S1-protected fragments; lane 2, G markers generated by guanine-specific cleavage of the hybridization probe. The correspondence between bands on the autoradiogram and the deduced position on the DNA sequence, as reported in Fig. 4, is shown. The 5' end of the mRNA is heterogeneous starting with either the A or the C nucleotide at positions 322 and 323.

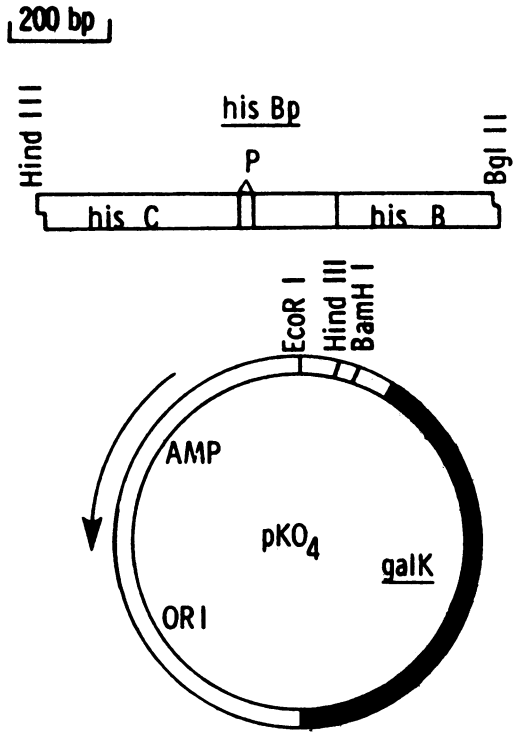

FIG. 6. The vector plasmid and derivative used to study promoter function. Circular map (not to scale) of the vector pKO4 and linear map of the 665-bp *Hin*dIII-*Bgl*II fragment containing the *hisBp* promoter cloned in the *Hin*dIII-*Bam*HI sites of pKO4. For further details of the construction of the recombinant plasmid pHC665, see the text. ORI, Origin of replication; AMP, ampicillin resistance gene; p, promoter.

acid sequence is in very good agreement with the rules governing codon usage in *E. coli* for biosynthetic gene products (17).

Expression of the distal histidine genes is controlled by both the primary *hisGp* promoter and by an internal transcription initiation site (1, 11, 18). Recently, Schmid and Roth (29) have conducted a detailed genetic analysis of the location of the internal promoters in *S. typhimurium* and have mapped the *hisBp* promoter at the end of the *hisC* gene. We previously mapped this site in the *Hin*dIII-*Bgl*II 665-bp fragment (18), the sequence of which is reported here. We

TABLE 4. Levels of galactokinase in *E. coli* N100 harboring different plasmids

Strain	Relevant genotype	Galactokinase level[a]		
		LB	Minimal medium	Minimal medium + AT 20 mM[b]
FB267	N100(pKO4)	0	7	NT
FB268	N100(pKG1800) (*galEp*)	NT	433[c]	NT
FB269	N100(pAR1) (*hisGp*)	75.3	510	1,500
FB270	N100(pHC665) (*hisBp*)	32.4	72.6	60

[a] Galactokinase specific activity is expressed as described by Mc Kenney et al. (26).
[b] See footnote *b* of Table 2. NT, Not tested.
[c] The strain was grown in minimal medium containing 1% Casamino Acids.

have now determined by S1 mapping and sequence analysis (Fig. 5) that the 5′ end of the mRNA is heterogeneous and that transcription initiates at nucleotides 322 to 323 (see above and Fig. 4). Inspection of the sequence upstream of this point shows sequences compatible with RNA polymerase-binding sites at a −35 region (TTTAAA versus TTGACA; nucleotides 290 to 295) and a −10 Pribnow box (CATTAT versus TATAAT; nucleotides 313 to 318) (28). The *hisBp* promoter is therefore localized in the distal portion of the *hisC* gene, in a manner similar to that of the *trpAp* internal promoter localized in the distal portion of the *trpD* gene (37).

The elegant system developed by Mc Kenney and colleagues to study promoter signals (26) was used to measure the efficiency of the *hisBp* promoter under several physiological conditions. Under repressed conditions in rich medium, the *hisBp* promoter was about 50% as efficient as the primary *hisGp* promoter cloned in plasmid pAR1 (Table 4) and hence slightly less efficient than the internal *trpAp* promoter responsible for 60 to 80% of the levels of the distal gene products (37). The internal *hisBp* promoter was also subject to metabolic regulation, as previously observed in *S. typhimurium* (36), albeit not at the same rate as the primary *hisGp* promoter, the levels of which increased sevenfold switching from rich to minimal medium compared with a twofold increase for the *hisBp* promoter (Table 4). Contrary to the primary *hisGp* promoter, the *hisBp* promoter was also not subject to histidine-specific regulation. The relative efficiencies of the *hisBp* promoter versus the *hisGp* promoter in the pKO4 system under different growth conditions are in rather good agreement with published in vivo levels of the histidine biosynthetic enzymes, both in minimal medium (11, 29) and under derepressed conditions (36).

Inspection of the sequence distal to the 5′ terminus of the mRNA responsible for the expression of the distal *his* genes revealed that the only open reading frame to the end of the fragment started with an ATG codon at nucleotide 430, approximately 100 bases after the 5′ end of the message. It is tempting to speculate that this amino acid sequence, which is in good agreement with the codon usage in *E. coli* (17), represents the beginning of the *hisB* gene product, also because this methionine codon is the only one preceeded by a Shine-Dalgarno box (GGAG; nucleotides 418 to 421) (31). If this were the case, the boundary between *hisC* and *hisB* would be constituted by a chain termination codon that overlaps the initiator codon by one nucleotide. This juxtaposition of translational signals occurs frequently in bacterial operons; it has been found, for instance, for the intercistronic regions between *trpE* and *trpD* and *trpB* and *trpA* (37) and may be important in dictating efficient initiation of translation (30).

Finally, we also showed that the entire histidine operon of *E. coli* K-12 resides on two contiguous *Hin*dIII fragments of the chromosome which have a total length of 9,800 bp. With our results and previous data (7, 10, 13, 18, 34), we were able to construct a complete restriction map of the *his* operon and to establish the relative position of the histidine genes (Fig. 1). The size of the entire operon, from the beginning of transcription at the *hisGp* promoter, does not exceed 7,600 bp. Very similar estimates have also been made for the *S. typhimurium* histidine operon (M. S. Carlomagno, F. Blasi, and C. B. Bruni, unpublished data). The six distal histidine genes *hisBHAFIE* are therefore contained in approximately 3,800 nucleotides, that is, an average of only 650 bp per gene. This region must possess a very compact organization. Sequence analysis and estimation of the size of the translation products in in vitro systems are currently in progress and will help elucidate these aspects.

ACKNOWLEDGMENTS

We thank M. Rosenberg for providing strains and plasmids and F. Blasi, R. Di Lauro, and V. E. Avvedimento for interest and criticism. A.R. is very grateful to M. Rosenberg for his kind interest and advice during a prolonged visit to his laboratory.

This work was supported in part by a grant from the Proggetto Finalizzato Ingegneria Genetica of the C.N.R.

LITERATURE CITED

1. **Atkins, J. F., and J. C. Loper.** 1970. Transcription initiation in the histidine operon of *S. typhimurium*. Proc. Natl. Acad. Sci. U.S.A. **65**:925–932.
2. **Bachmann, B. J., and K. B. Low.** 1980. Linkage map of *Escherichia coli* K-12, edition 6. Microbiol. Rev. **44**:1–56.
3. **Bickle, T. A., V. Pirrotta, and R. Imber.** 1977. A simple general procedure for purifying restriction endonucleases. Nucleic Acids Res. **4**:2561–2572.
4. **Blasi, F., and C. B. Bruni.** 1981. Regulation of the histidine operon: translation controlled transcription termination. A mechanism common to several biosynthetic operons. Curr. Top. Cell. Regul. **19**:1–45.
5. **Bolivar, R., R. L. Rodriguez, M. C. Betlach, and H. W. Boyer.** 1977. Construction and characterization of new cloning vehicles. I. Ampicillin resistance derivatives of the plasmid pMB9. Gene **2**:75–93.
6. **Brenner, M., and B. N. Ames.** 1971. The histidine operon and its regulation, p. 349–387. *In* H. S. Vogel (ed.), Metabolic pathways, vol. 5. Academic Press, Inc., New York.
7. **Bruni, C. B., A. M. Musti, R. Frunzio, and F. Blasi.** 1980. Structural and physiological studies of the *Escherichia coli* histidine operon inserted into plasmid vectors. J. Bacteriol. **142**:32–42.
8. **Clewell, D. B.** 1972. Nature of ColE1 plasmid replication in *Escherichia coli* in the presence of chloramphenicol. J. Bacteriol. **110**:667–676.
9. **Davis, R. W., D. Botstein, and J. R. Roth.** 1980. Advanced bacterial genetics, p. 116–125. Cold Spring Harbor Laboratory, Cold Spring Harbor, N.Y.

10. **Di Nocera, P. P., F. Blasi, R. Di Lauro, R. Frunzio, and C. B. Bruni.** 1978. Nucleotide sequence of the attenuator region of the histidine operon of *Escherichia coli* K-12. Proc. Natl. Acad. Sci. U.S.A. **75**:4276–4280.
11. **Ely, B., and Z. Ciesla.** 1974. Internal promoter P2 of the histidine operon of *Salmonella typhimurium*. J. Bacteriol. **120**:980–986.
12. **Favaloro, J., R. Treisman, and R. Kamen.** 1980. Transcription maps of polyoma virus-specific RNA: analysis by two-dimensional nuclease S1 gel mapping. Methods Enzymol. **65**:718–749.
13. **Frunzio, R., C. B. Bruni, and F. Blasi.** 1981. *In vivo* and *in vitro* detection of the leader RNA of the histidine operon of *Escherichia coli* K-12. Proc. Natl. Acad. Sci. U.S.A. **78**:2767–2771.
14. **Garrick-Silversmith, L., and P. E. Hartman.** 1970. Histidine requiring mutants of *Escherichia coli* K-12. Genetics **66**:231–244.
15. **Goldschmidt, E. P., M. S. Cater, T. S. Matney, M. A. Butler, and A. Greene.** 1970. Genetic analysis of the histidine operon in *Escherichia coli* K-12. Genetics **66**:219–229.
16. **Gordon, J. F., R. G. Deeley, A. T. H. Burns, B. M. Paterson, J. L. Christmann, and R. F. Goldberger.** 1977. Primary activation of the vitellogenin gene in the rooster. J. Biol. Chem. **252**:8310–8319.
17. **Gouy, M., and C. Gautier.** 1982. Codon usage in bacteria: correlation with gene expressivity. Nucleic Acids Res. **10**:7055–7074.
18. **Grisolia, V., M. S. Carlomagno, and C. B. Bruni.** 1982. Cloning and expression of the distal portion of the histidine operon of *Escherichia coli* K-12. J. Bacteriol. **151**:692–700.
19. **Hershfield, V., H. W. Boyer, C. Yanofsky, M. A. Lovett, and D. R. Helinsky.** 1974. Plasmid ColE1 as a molecular vehicle for cloning and amplification of DNA. Proc. Natl. Acad. Sci. U.S.A. **71**:3455–3459.
20. **Kasai, T.** 1974. Regulation of the expression of the histidine operon in *Salmonella typhimurium*. Nature (London) **249**:523–527.
21. **Lowry, O. J., N. J. Rosebrough, A. L. Farr, and R. J. Randall.** 1951. Protein measurement with the Folin phenol reagent. J. Biol. Chem. **193**:265–275.
22. **Maniatis, T., E. F. Fritsch, and J. Sambrook.** 1982. Molecular cloning, p. 164. Cold Spring Harbor Laboratory, Cold Spring Harbor, N.Y.
23. **Martin, R. G., M. A. Berberich, B. N. Ames, W. W. Davis, R. F. Goldberger, and J. D. Yourno.** 1971. Enzymes and intermediates in the histidine biosynthesis of *Salmonella typhimurium*. Methods Enzymol. **17B**:3–44.
24. **Martin, R. G., M. J. Voll, and E. Appella.** 1967. Imidazolylacetolphosphate:L-glutamate aminotransferase. Composition and substructure. J. Biol. Chem. **242**:1175–1181.
25. **Maxam, A. M., and W. Gilbert.** 1980. Sequencing end-labeled DNA with base-specific chemical cleavages. Methods Enzymol. **65**:499–560.
26. **Mc Kenney, K., H. Shimatake, D. Court, U. Schmeissner, C. Brady, and M. Rosenberg.** 1981. A system to study promoter and terminator signals recognized by *Escherichia coli* RNA polymerase, p. 383–415. *In* J. G. Chirichjian and T. S. Papas (ed.), Gene amplification and analysis, vol. 2, Analysis of nucleic acids by enzymatic methods. Elsevier/North-Holland, New York.
27. **Miller, J. H.** 1972. Experiments in molecular genetics, p. 433. Cold Spring Harbor Laboratory, Cold Spring Harbor, N.Y.
28. **Rosenberg, M., and D. Court.** 1979. Regulatory sequences involved in the promotion and termination of RNA transcription. Annu. Rev. Genet. **13**:319–353.
29. **Schmid, M. B., and J. H. Roth.** 1983. Internal promoters of the *his* operon in *Salmonella typhimurium*. J. Bacteriol. **153**:1114–1119.
30. **Schümperly, D., K. Mc Kenney, D. A. Sobieski, and M. Rosenberg.** 1982. Translational coupling at an intercistronic boundary of the *Escherichia coli* galactose operon. Cell **30**:865–871.
31. **Shine, J., and L. Dalgarno.** 1974. The 3'-terminal sequence of *Escherichia coli* 16S ribosomal RNA: complementarity to nonsense triplets and ribosome binding sites. Proc. Natl. Acad. Sci. U.S.A. **71**:1342–1346.
32. **Sollner-Webb, B., and R. H. Reeder.** 1979. The nucleotide sequence of the initiation and termination sites for ribosomal RNA transcription in *X. leavis*. Cell **18**:485–499.
33. **Staples, M. A., and L. L. Houston.** 1979. Proteolytic degradation of imidazoleglycerolphosphate dehydratase-histidinol phosphatase from *Salmonella typhimurium* and the isolation of a resistant bifunctional core enzyme. J. Biol. Chem. **254**:1395–1401.
34. **Verde, P., R. Frunzio, P. P. Di Nocera, F. Blasi, and C. B. Bruni.** 1981. Identification, nucleotide sequence, and expression of the regulatory region of the histidine operon of *Escherichia coli* K-12. Nucleic Acids Res. **9**:2075–2086.
35. **Vogel, H. J., and D. M. Bonner.** 1956. Acetyl ornithase of *Escherichia coli*: partial purification and some properties. J. Biol. Chem. **218**:97–106.
36. **Winkler, M. E., D. J. Roth, and P. E. Hartman.** 1978. Promoter- and attenuator-related metabolic regulation of the *Salmonella typhimurium* histidine operon. J. Bacteriol. **133**:830–843.
37. **Yanofsky, C., T. Platt, I. P. Crawford, B. P. Nichols, G. E. Christie, H. Horowitz, M. VanCleemput, and A. M. Wu.** 1981. The complete nucleotide sequence of the tryptophan operon of *Escherichia coli*. Nucleic Acids Res. **9**:6647–6668.